frontiers in Chemical Engineering

ORIGINAL RESEARCH
published: 11 November 2021
doi: 10.3389/fceng.2021.756026

N_2O–Assisted Siphon Foaming of Modified Galactoglucomannans With Cellulose Nanofibers

Tiina Nypelö[1,2], Jessica Fredriksson[1], Vishnu Arumughan[1], Emanuel Larsson[3,4], Stephen A. Hall[4,5] and Anette Larsson[1,2]**

[1]Applied Chemistry, Department of Chemistry and Chemical Engineering, Chalmers University of Technology, Gothenburg, Sweden, [2]Wallenberg Wood Science Center, Chalmers University of Technology, Gothenburg, Sweden, [3]RISE Research Institutes of Sweden, Lund, Sweden, [4]Division of Solid Mechanics, Lund University, Lund, Sweden, [5]Lund Institute of Advanced Neutron and X-ray Science, Lund, Sweden

Foaming of most bio-based polymers is challenged by low pore formation and foam stability. At the same time, the developing utilization of bio-based materials for the circular economy is placing new demands for easily processable, low-density materials from renewable raw materials. In this work, we investigate cellulose nanofiber (CNF) foams in which foaming is facilitated with wood-based hemicelluloses, galactoglucomannans (GGMs). Interfacial activity of the GGM is modulated *via* modification of the molecule's amphiphilicity, where the surface tension is decreased from approximately 70 to 30 mN m^{-1} for unmodified and modified GGM, respectively. The chemical modification of GGMs by substitution with butyl glycidyl ether increased the molecule's hydrophobicity and interaction with the nanocellulose component. The highest specific foam volume using 1 wt% CNF was achieved when modified GGM was added (3.1 ml g^{-1}), compared to unmodified GGM with CNF (2.1 ml g^{-1}). An amount of 96 and 98% of the GGM and GGM-BGE foams were lost after 15 min of foaming while the GGM and GGM-BGE with cellulose nanofibers lost only 33 and 28% of the foam respectively. In the case of GGM-BGE, the foam stability increased with increasing nanofiber concentration. This suggests that the altered hydrophobicity facilitated increased foam formation when the additive was incorporated in the CNF suspension and foamed with nitrous oxide (N_2O). Thus, the hydrophobic character of the modified GGM was a necessity for foam formation and stability while the CNFs were needed for generating a self-standing foam structure.

Keywords: galactoglucomannan, cellulose nanofibers, polysaccharide interactions, foaming, interfacial interactions

OPEN ACCESS

Edited by:
Vincenzo Russo,
University of Naples Federico II, Italy

Reviewed by:
Nguyen Van Duc Long,
Yeungnam University, South Korea
Maria Lucia Caetano Pinto Da Silva,
University of São Paulo, Brazil

****Correspondence:***
Jessica Fredriksson
jessica.fredriksson.94@gmail.com
Anette Larsson
anette.larsson@chalmers.se

Specialty section:
This article was submitted to Chemical Reaction Engineering, a section of the journal Frontiers in Chemical Engineering

Received: *09 August 2021*
Accepted: *29 September 2021*
Published: *11 November 2021*

Citation:
Nypelö T, Fredriksson J, Arumughan V, Larsson E, Hall SA and Larsson A (2021) N_2O–Assisted Siphon Foaming of Modified Galactoglucomannans With Cellulose Nanofibers. Front. Chem. Eng. 3:756026. doi: 10.3389/fceng.2021.756026

1 INTRODUCTION

All-wood foams are of great interest in terms of the quest for easily processable, low-density materials from renewable raw materials as part of the circular economy. However, the production of these materials is also one of the key challenges of the forest products community. The benefit of wood foams over the synthetic plastics, such as polyurethanes, is their renewable raw material. Foaming of synthetic polymers is facilitated using chemical or physical blowing agents and often thermal processes (Soykeabkaew et al., 2015; Marrazzo et al., 2016; Gama et al., 2018). This production approach is also employed for some bio-based polymers; however, the restricted thermo-moldability

and solubility of most of them is a limitation (Hillis, 1984; Cosgrove, 2005; Jeon et al., 2013; Marrazzo et al., 2016). Alternatively, some polysaccharides, such as starch and cellulose derivatives, can be foamed in extrusion by utilizing water as the blowing agent (Chinnaswamy, 1993; Hofmann et al., 1998; Cha et al., 2001; Karlsson et al., 2015). Furthermore, cellulose and hemicellulose are typically transformed into foams by controlled drying of hydrogels that is often performed via lyophilization (Kistler, 2002; Sehaqui et al., 2010).

The usage of siphons in food processing is an established technique to create foams (Getz et al., 1937; Blankart et al., 2020). The foam production is achieved by incorporating liquid N_2O into the foam precursor that is then dispensed through a nozzle. This leads to the expansion of N_2O and formation of wet foam. N_2O, which dissolves readily in both hydrophilic and hydrophobic substances (such as water and oil; O'Neil et al., 2001), has a larger solubility in olive oil than CO_2 (Yokozeki and Shiflett, 2011) and is a nontoxic noncarcinogenic substance. It dissolves readily in fat and has been reported to enable film formation around the generated gas bubbles (Stankov et al., 2021). The use of this foaming technique is common in food production, but the siphon foaming has also been suggested for engineered materials, e.g., silk fibroin scaffold preparation (Maniglio et al., 2018).

Nanocellulose refers to nanosized particles that are liberated from plant cell walls (Dufresne, 2012; Dufresne, 2013). Cellulose nanofibers (CNF) have emerged as a potential material for making foams due to that the nanosized fibrils form dry foams with small pores and high density, and the strong fibril network contributes to strength (Svagan et al., 2008; Sehaqui et al., 2010; Sehaqui et al., 2011; Cervin et al., 2013; Martoïa et al., 2016; Lavoine and Bergström, 2017; Antonini et al., 2019) that can surpass wood macrofiber foam properties (Kuboki et al., 2009; Xie et al., 2011; Kuboki, 2014; Ottenhall et al., 2018). The common method to transfer nanocelluloses into foams is by the removal of solvent from nanocellulose suspension, which leads to the formation of a porous fibril network (Ganesan et al., 2018). Foaming of nanocelluloses can also be realized by incorporating a foaming agent in the suspension and is followed with freeze-drying (Wemmer et al., 2019). However, the nanocelluloses are more commonly known for stabilizing emulsions than foams (Fujisawa et al., 2017). This difference has been attributed to the unfavorable contact angle and reversible adsorption at the air–water interface (Bergfreund et al., 2019; Bertsch et al., 2019; Bertsch and Fischer, 2020). The stabilization action of the CNF in foams has been found to be better than that of another nanocellulose grade, cellulose nanocrystals, and this benefit was identified as being due to the higher aspect ratio of CNFs which favors network formation at particle-filled air–water interfaces (Cervin et al., 2015; Capron et al., 2017).

Wood hemicelluloses are a grade of polysaccharides and comprise a linear backbone with xylose in hardwoods and glucose and mannose in softwoods. They also contain side groups of glucuronic acid in hardwoods and galactose in softwoods (Ebringerová, 2005). The backbone can be partly acetylated or contain residual amounts of lignins that alter hydrophilicity (Lawoko, 2013; Maleki et al., 2017). Despite

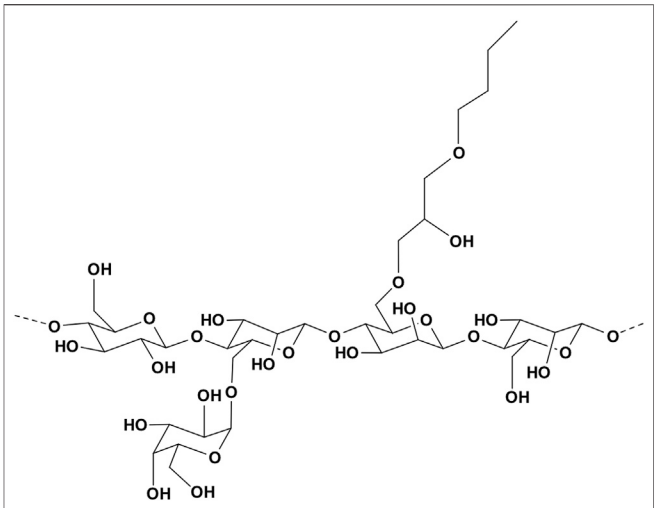

FIGURE 1 | Schematic presentation of galactoglucomannan modified with a hydrophobic side chain.

that the surface activity of wood glucomannans is often modest (Xu et al., 2007), they have been demonstrated to stabilize beverage emulsions (Mikkonen et al., 2009) as well as oil-in-water emulsions (Lehtonen et al., 2016; Mikkonen et al., 2016). Most of the studies suggest that stabilization is enabled by the hydrophobic moieties, such as wood-derived phenolic residues, or may be related to Pickering-type stabilization by polysaccharide colloidal assemblies (Lehtonen et al., 2018).

For the first time, this study uses siphon and N_2O to form wood-based foams consisting of CNFs and galactoglucomannans (GGMs) to provide enhanced foam formation and stability of CNF foams. The motivating hypothesis for this approach is that the increase in interfacial activity is a prerequisite for the foam formation. Therefore, the surface activity of the GGM is expected to be increased by hydrophobic derivatization. We hypothesize that this leads to increased foam stability due to its higher interfacial activity and interaction with N_2O that is known to be oil-soluble.

2 EXPERIMENTAL

2.1 Materials

The GGM investigated in this study was isolated from thermomechanical pulp received from Stora Enso (Kvarnsveden, Sweden) and ultrafiltered using 5 kDa membranes. The GGM concentration prior to ultrafiltration was less than 1% w/w. The solid GGM was achieved by precipitation using 95% ethanol (Solveco, Rosersberg, Sweden) in a 2:1 ratio, centrifuged, dried in room temperature, and stored for further usage (Willför et al., 2003). The GGM was modified by hydrophobic side chains, butyl glycidyl ether (BGE; Nypelö et al., 2016) (**Figure 1**). NaOH pellets (VWR, Sweden) were added to 436 g GGM solution (10% w/w) in mol equivalent to 3:1 NaOH to GGM monomer. BGE, purchased from Sigma-Aldrich (St. Louis, MO, United States), was added dropwise under an inert

atmosphere in mol equivalent to 3:1 BGE to GGM monomer, and the solution stood overnight in a 45°C oil bath under magnetic stirring. The solution was then neutralized and dialyzed for approximately 1 week using a Spectra/Por 7 Dialysis membrane with a molecular weight cutoff of 1 kDa (Spectrum Laboratories, Rancho Dominguez, CA, United States). The CNF from softwood via enzymatic pretreatment was received from Stora Enso (Karlstad, Sweden) as a slurry (4.2 wt%). The bleached softwood kraft pulp has a typical glucose content of 85% (Sixta, 2006).

2.2 Foaming and Drying

The concentration of the solutions containing GGM was kept constant at 6 wt% and cellulose nanofiber suspensions were added to give 0, 0.2, 0.4, 1, and 2 wt% cellulose nanofiber concentration. The foaming procedure was performed on mixtures containing nanofibers and GGM/modified GGM using 0.5 L siphon (Exxent, Sweden) and 8 g nitrous oxide gas patrons (Exxent, Sweden) in plastic tubes for 30 s. Thereafter, the foams were frozen and freeze-dried (FreeZone®, Labconco, US) at −40°C for 5 days and stored in a desiccator for further analyses.

2.3 Compositional Characterization

The GGM has been characterized by Härdelin et al. (2020). The main carbohydrates in the GGM were galactose, glucose, and mannose, with an average molar ratio of 1:1.4:4.6. The molecular weight (Mw) was 15 kDa. The molar substitution of BGE was reported to be 2.1 (Härdelin et al., 2020). Fourier transform infrared spectroscopy (FTIR) analysis of the GGM grades is presented in **Supplementary Figure S1**.

2.4 Solution and Interfacial Characterization

Solutions of the modified and unmodified GGMs (1 mg ml^{-1}) were analyzed with dynamic light scattering (DLS) (Beckman Coulter N4 Plus submicron particle size analyser), with 90° scattering angle, 5 min measuring time, and at a temperature of 23°C and reported as number-based distribution.

The surface tension was determined by using an Attension Theta optical tensiometer (KSV instruments, Biolin Scientific, Sweden) and pendant drop shape analysis. The shape was recorded immediately after the maximum drop size was achieved.

Adsorption of the hemicelluloses, both modified and unmodified GGMs, on the CNF were analyzed using a quartz crystal microbalance with dissipation monitoring (QCM-D, Q-Sense AB Gothenburg, Sweden) at a temperature of 22°C. The CNF substrates were prepared following a reported procedure (Palasingh et al., 2021). First SiO_2-coated QCM-D sensors were cleaned by immersion in 10% NaOH solution for 20 s, rinsed with excess of water, and dried with nitrogen gas. The cleaned sensor was then immersed in 1.6 g L^{-1} of PEI solution to deposit a positively charged anchoring layer. The spin-coating solution was prepared by dispersing CNFs in water (1.7 g L^{-1}) by ultrasound sonication (Sonics VCX-750 Vibra-Cell Ultra sonicator) for 5 min (20% power). The dispersion was then centrifuged for 40 min in 6,000 rpm (Beckman Coulter Optima XL-100K ultracentrifuge). The supernatant was used for spin coating using 3,000 rpm, with an acceleration of 2,100 rpm s^{-1} for 1 min (SPS Spin 150). The films were then treated in an oven for 10 min at 80°C and stored in a desiccator.

2.5 Rheological Characterization

The rheological behavior of unmodified and modified GGM, with or without the nanocellulose, was analyzed using a Discovery Hybrid Rheometer 3 (TA Instruments). The concentrations of unmodified and modified GGM without nanofibers were between 0.2 and 2.0 wt%. The concentration of unmodified and modified GGM was fixed at 6 wt%, when combined with nanofibers, and the concentration of nanocellulose varied between 0 and 2.0 wt%. The measurements were performed at 25°C using the following procedure: first run at 10.0 s^{-1} for 60 s; thereafter, the shear rate was immediately decreased to 0.03 s^{-1} and then ramped up to 1,000 s^{-1} and then decreased from 1,000 to 0.03 s^{-1}.

2.6 Foam Volume Determination

To assess the foam stability, the foam and the precursor suspension volumes were determined volumetrically as a function over time for 125 min and used for calculating the foam specific volume (V), determined as the foam volume in relation to the initial total mass. Lost volume, V_L, was determined after 15 min as the volume% of the solution that was incorporated in the foam.

3 RESULTS

3.1 N_2O–Assisted Foaming

N_2O is soluble in hydrophilic and hydrophobic substances (O'Neil et al., 2001; Yokozeki and Shiflett, 2011; Stankov et al., 2021) and hence used for foaming of hydrophobic substances in hydrophilic matrices (e.g., water). Here, we used foaming aided by N_2O following a traditional siphon foaming approach of incorporating liquid N_2O into an aqueous foam precursor in a container (**Figures 2A–C**). The aqueous foam precursors contained GGM, GGM-BGE alone, or a CNF suspension. The release of the foam precursors containing N_2O (aq) under ambient conditions led to the expansion of N_2O into gas (g) and formation of a foam (**Figure 2D**).

The hypothesis of this work was that a hydrophobic component is required to facilitate foaming and foam stability. The GGM did not decrease the surface tension of water–air interface. However, the GGM-derivative containing the aliphatic modification (**Figure 1**), i.e., the GGM-BGE, decreased the surface tension to 30 mN m^{-1} (**Figure 3**). These findings comply with the previous work (Nypelö et al., 2016) and indicate that the modified GGM was successfully functionalized with aliphatic side chains, which alters the polarity of the molecule resulting in increased interfacial activity of the molecule in aqueous environment.

Light scattering revealed that the GGM solution (1 mg ml^{-1}) contains structures with a hydrodynamic diameter of 1.3 ± 0.1 nm and the GGM-BGE solution, 87.0 ± 36.6 nm. Wood hemicellulose water solubility depends on their source and the substituting units and degree of substitution, and hence the detectable features in the DLS analysis, are not surprising

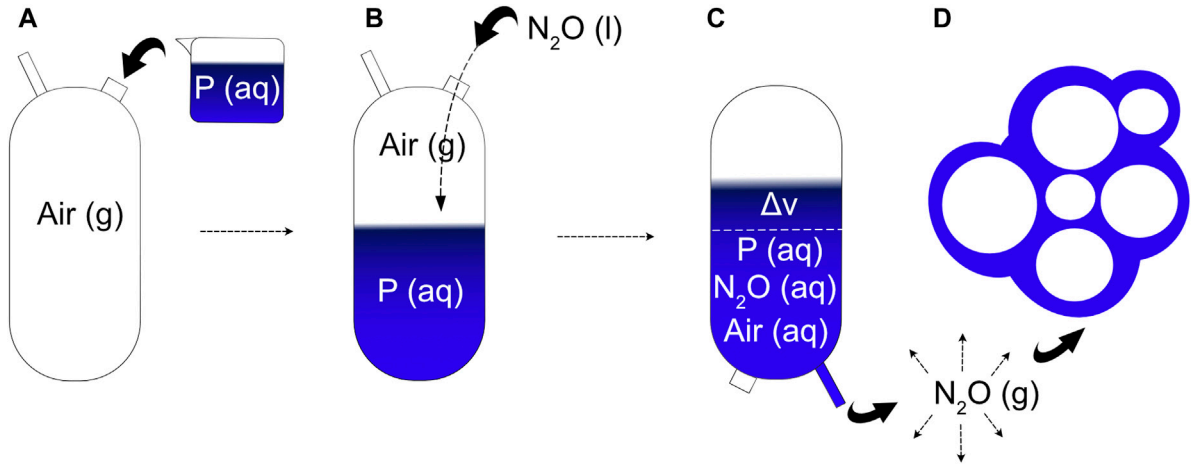

FIGURE 2 | Schematic presentation of foaming with nitrous oxide (N_2O). **(A)** A container is filled with a foam precursor P, in this study, containing CNF and GGM or GGM-BGE in water (aq). **(B)** Liquid (l) N_2O is fed into the container and **(C)** it is absorbed into the foam precursor. This leads to increase in volume (v) due to the incorporation of N_2O. **(D)** Inversion of the container and release of the foam precursors containing N_2O (l) lead to expansion of N_2O into gas (g) and formation of a foam. Surface tension and solubility of the GGM and GGM-BGE systems.

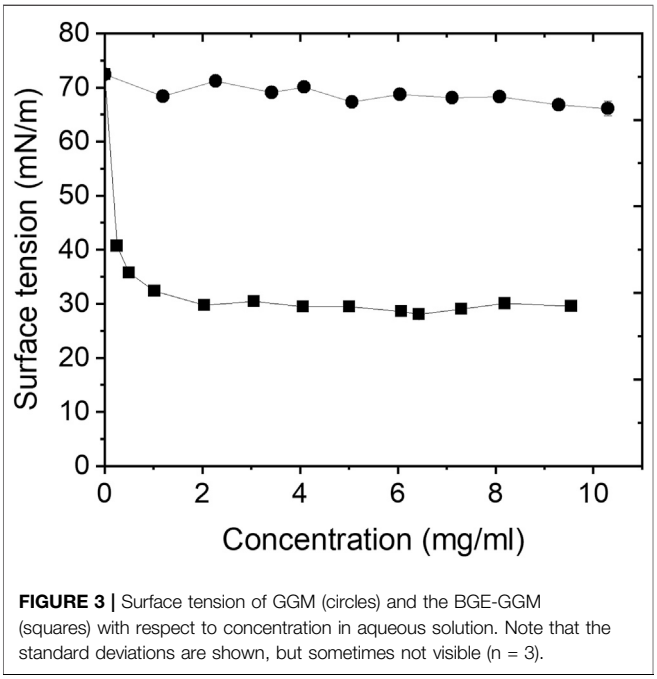

FIGURE 3 | Surface tension of GGM (circles) and the BGE-GGM (squares) with respect to concentration in aqueous solution. Note that the standard deviations are shown, but sometimes not visible (n = 3).

(Kishani et al., 2018). However, the GGM-BGE clearly features aggregation that we deem to originate from the reduction of its water solubility.

3.2 Wet Foam Stability

Foam stability of neat GGM and GGM-BGE and both in the presence of CNF was elaborated by analysis of the foam specific volume V and lost foam volume V_L. The specific volume is the ratio of the volume of the foam to the mass of the precursor at time zero and was lower for GGM than for GGM-BGE (2.4 vs. 3.0 ml g^{-1}), indicating a low foaming capacity of GGM compared to that of GGM-BGE (**Table 1**). We note that although the surface tension analysis (**Figure 1**) did not indicate the GGM to be interfacially active, foams could also be formed with the GGM, even though with lower V. An amount of 96% of the GGM-BGE foam was lost after 15 min, being on similar level with the value for GGM that was 98%. Hence, both the GGM and GGM-BGE foams were found to be unstable with time.

TABLE 1 | Foam specific volume (V) and lost foam volume (V_L) of the formulations.

Foam	V (ml g^{-1})	V_L (%)
GGM	2.4	98
GGM-CNF 1 wt%	2.1	33
GGM-BGE	3.0	96
GGM-BGE-CNF 1 wt%	3.1	28
CNF 1 wt%	1.2	33

The specific volume V for the GGM-CNF foams was approximately the same as that of GGM alone (2.1 vs. 2.4 ml g^{-1}), indicating insignificant influence of the CNF to the foaming ability. However, the lost foam volume (**Table 1**) of GGM foam was 98% while for GGM-CNF it was only 33%, which indicates more stable foam being generated with CNFs. The reference foam prepared using 1 wt% CNF had the lowest specific volume (1.2 ml g^{-1}). Although only 33% of the foam was lost after 15 min, we note that the foam had a gel-like character, being different from the other foams (**Supplementary Figure S2**). The appearance of the foams after 15 min is presented in **Supplementary Figures S2, S3**.

Incorporation of CNFs to the GGM-BGE led to the highest foam specific volume (3.1 ml g^{-1}) and the lowest lost foam

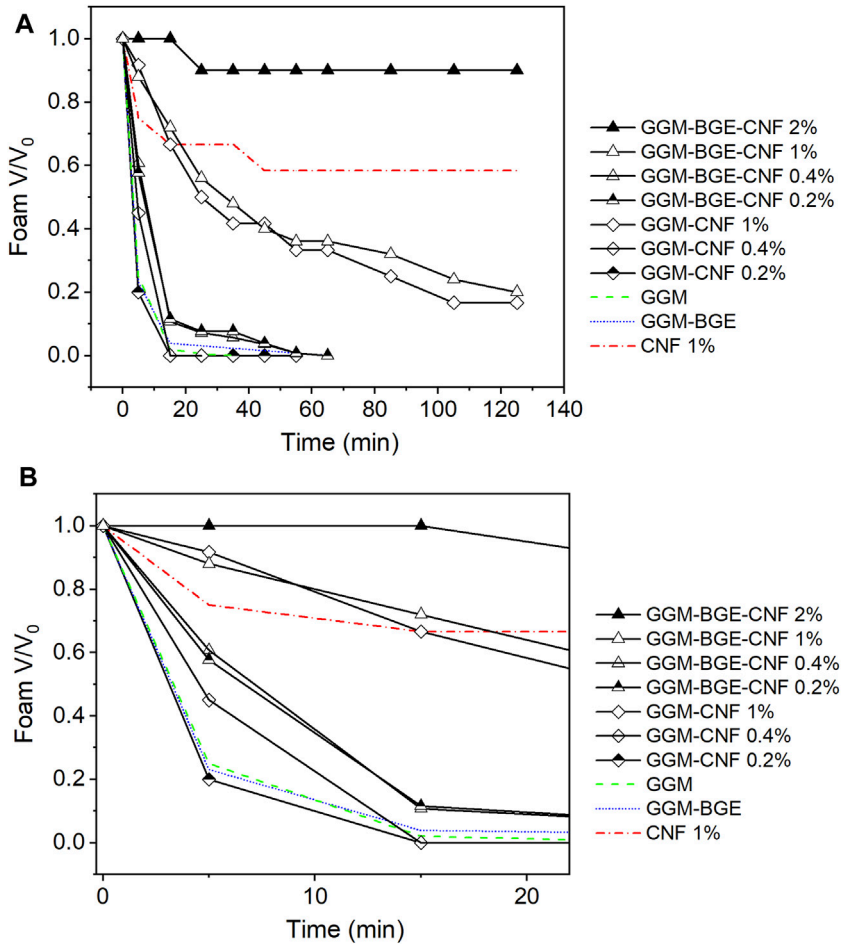

FIGURE 4 | (A) Foam stability as the foam specific volume V in comparison to the initial foam specific volume V_0 with respect to CNF concentration for selected foam grades. **(B)** Inset. The Foam of GGM-CNF 2% could not be formed and is not shown.

volume, 28%. It appears that hydrophobic components in the foam formulation led to larger foam volumes. Since N_2O is known to be soluble in hydrophobic matrices (Yokozeki and Shiflett, 2011) and to solubilize hydrophobic components, it may be an underlying factor contributing to the highest foam volume fractions of the foams with hydrophobic components. We speculate that these formulations may be able to incorporate more N_2O (larger Δv in **Figure 2C**) and hence lead to the highest specific volumes (**Table 1**).

The foam stability of the wet foams is presented as the foam specific volume (V) at given points of time in comparison to the initial (at 0 min) foam specific volume (V_0) over an observation period of 125 min (**Figure 4**). The foams with GGM and the GGM-BGE alone collapsed after 15 min, while the pristine CNF foam decreased until reaching a plateau of 45 min after the foaming.

The GGM-stabilized CNF foams, with the lowest CNF concentration of 0.2 wt%, were as unstable as the neat GGM foams (**Figures 4A, B**). Increase in the CNF concentration to 0.4 and 1 wt% increased the stability, but with 2 wt% CNF increase the foam could not be formed. In the case of the GGM-BGE-CNF foams, the stability increased with increasing CNF concentration. We observe that while the stability of the foams appears equal with 1 wt% CNF concentration for both GGM and GGM-BGE, the increase in the CNF concentration in the foam from 1 to 2 wt % resulted in it not being possible to form a foam when using GGM as the foaming additive, but the foam stability increased for GGM-BGE. The presence of the hydrophobic component seems to be essential for an increase both in foam volume and in the foam stability. The observation during foaming was that the incorporation of CNF into the GGM made the system thicker and hence making foaming in the siphon challenging, which led to larger gas bubbles and, presumably, also to foam instability.

The CNF foam appeared to perform well when the stability over the 125 min period was scrutinized (**Figure 4**). To further inspect the stability, an investigation of the specific volume V compared to the initial foam mass was performed (**Figure 5**).This presentation amplifies the stability with respect to the amount of the precursor that was attempted to be foamed, rather than only considering the amount of the formed foam that was retained. In

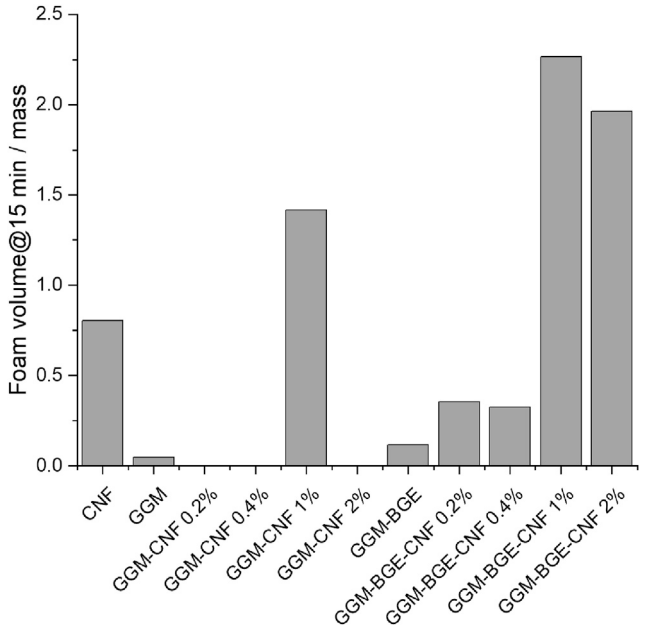

FIGURE 5 | Foam stability elucidated by contrasting foam specific volume at a given time of observation to the initial mass of the precursor suspension.

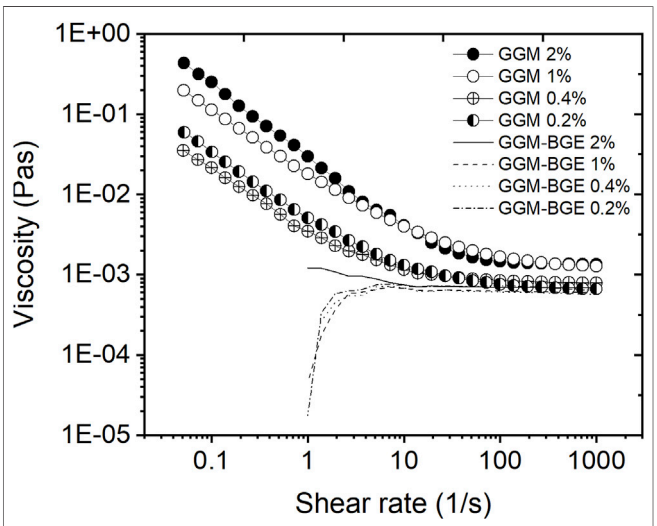

FIGURE 6 | Viscosity as function of the shear rate of systems containing 0.2 to 2.0 wt% GGM (circle symbols) and GGM-BGE (lines).

this consideration, the CNF performance decreases, in comparison to when accompanied with the hemicellulose additive, and it becomes evident that GGM-BGE additive is needed to facilitate efficient conversion of the precursor into a foam.

The siphon foaming occurs by depressurizing the precursor–N_2O suspension, abrupt instability, cell nucleation, and growth followed by stabilization of the foamed cellular

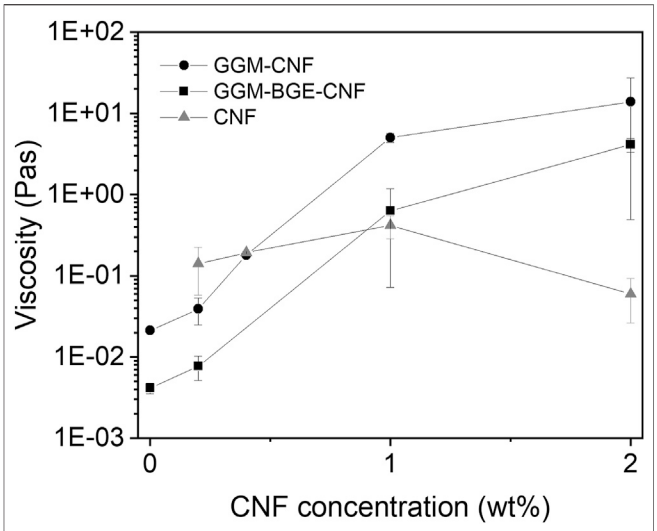

FIGURE 7 | Viscosity of systems with only CNF (gray filled triangles), 6 wt % GGM with 0–2 wt% CNF (circles), and 6 wt% GGM-BGE with 0–2 wt% CNF (squares) recorded at a shear rate of 1 s^{-1}.

structure. The latter steps are determined by the rheological characteristics of the solution and hence this characterization was performed. During the bubble growth, a low viscosity of the expanding matter allows elongation of the liquid surrounding the bubble, while, after the formation of foam bubbles, the cellular structure containing polymers leads to greater resistance to the stretching and prevents the collapse of the foamed structure. The viscosity of GGM solutions were higher at all investigated concentrations and exhibited non-Newtonian behavior, while the GGM-BGE solutions were Newtonian and had lower viscosity (**Figure 6**). This can be one of the reasons for the difficulty to foam the GGM in comparison to GGM-BGE. As expected, inclusion of CNF in solutions increased the viscosity for both the GGM and GGM-BGE solutions (**Figure 7**).

The wet foams were dried *via* freezing and lyophilization, which resulted in self-standing foams. The structural investigation of these foams is presented in **Supplementary Figures S4–S6**. The benefit of incorporation of GGM-BGE, rather than GGM, in the CNF foams was that the foams containing the former were able to withstand the forces (capillary, gravitational, and interfacial) created during the drying process to yield porous dry foams. The foams containing GGM suffered from artifacts caused by drying, which may be the result of the observed lower stability. We deem that the hydrophobicity of GGM was needed for foam formation while the cellulose fibrils were needed for generating a self-standing foam structure.

4 DISCUSSION

The question to answer is why does the GGM-BGE improve the foam stability (and porous dry foam structure) in the CNF matrix while

inclusion of GGM in CNF matrix leads to lower stability of the wet foam (**Figure 3**; see, e.g., 0.2 and 0.4% addition of CNF), as well as an inability to withstand the freezing and drying (**Supplementary Figures S5, S6**). The underlying reasons may be 1) the improved surface activity of the GGM by the BGE modification, 2) altered interactions between GGM and CNF, as a result of the GGM modification, 3) contribution of the CNF to the surface activity, or 4) higher affinity of N_2O to GGM-BGE than GGM, which facilitates more N_2O to be absorbed in the foam precursor.

Let us first consider reason 3. The surface tension of dilute CNF suspension was determined to be 69.6 mN m^{-1} (**Supplementary Table S1**), which does not imply a significant reduction in the surface tension of the solvent (water in this case). We also quantified the surface tension of mixtures of CNF with GGM and GGM-BGE. This is important because surface active molecules can show retarded reduction in surface energy if their diffusion to the interface is hindered (Beneventi et al., 2001). However, CNF did not cause this and the surface activity in the GGM and GGM-BGE containing CNF systems was not altered (**Supplementary Table S1**).

To elucidate reason 2 and indicate the attraction between CNF and unmodified and modified GGM, respectively, QCM-D was used. GGM showed a higher affinity to the CNF than GGM-BGE, indicated by a higher frequency change upon adsorption on the oscillating sensor that corresponded to 5.0 and 3.8 mg m^{-2} adsorbed mass. (The frequency response is presented in **Supplementary Figure S7**.) We conclude that the GGM is likely to adsorb on the CNF surface while in the case of the GGM-BGE the adsorbed fraction is lower leaving the GGM-BGE free to migrate to the bubble matrix interface during foaming, which may stabilize the foam. This tendency of stronger interactions between GGM without modifications and CNF is intrinsically driven by the difference in the polarity of the compounds or lower amount of released water giving lower entropic contribution. Determination of N_2O adsorption into the foam precursor to enable to state the contribution of reason 4) remains a future task, but could also be a factor making BGE-GGM-CNF foams more stable.

5 CONCLUSION

This study used siphon and N_2O to form wood-based foams consisting of CNFs and GGMs to provide enhanced foam formation and CNF foam stability. We conclude that the surface activity of the GGM by the BGE modification is an important factor for foaming efficiency of CNFs with a wood GGM grade. This has been shown by the increased specific volume of foams containing the modified GGM with lower surface tension (30 mN m^{-1}) compared to that of unmodified GGM (70 mN m^{-1}). The surface activity was introduced by modification of the GGM with an aliphatic side chain. Utilizing the modified glucomannan as an additive in a CNF suspension enabled a foam formation when siphon foaming using N_2O was applied and freeze-drying led to dry foams. Without the modification of the GGM, the wet foams were not able to withstand freezing and drying was required to transform them into porous dry foams.

DATA AVAILABILITY STATEMENT

The raw data supporting the conclusion of this article will be made available by the authors, without undue reservation.

AUTHOR CONTRIBUTIONS

JF performed majority of the experiment and analyzed the results; VA, EL, and SH performed part of the experiment and data analysis; and AL and TN helped in conceptualization, data interpretation, and writing the first draft. All authors wrote and revised the article.

ACKNOWLEDGMENTS

Stora Enso AB (Karlstad, Sweden) is acknowledged for providing the GGM and CNF. The authors acknowledge Wallenberg Wood Science Center and Forskningsrådet Formas and the Swedish research project SmartFoam for their financial support.

SUPPLEMENTARY MATERIAL

The Supplementary Material for this article can be found online at: https://www.frontiersin.org/articles/10.3389/fceng.2021.756026/full#supplementary-material

REFERENCES

Antonini, C., Wu, T., Zimmermann, T., Kherbeche, A., Thoraval, M.-J., Nyström, G., et al. (2019). Ultra-Porous Nanocellulose Foams: A Facile and Scalable Fabrication Approach. *Nanomaterials* 9, 1142. doi:10.3390/nano9081142

Beneventi, D., Carre, B., and Gandini, A. (2001). Role of Surfactant Structure on Surface and Foaming Properties. *Colloids Surf. A.* 189, 65–73. doi:10.1016/s0927-7757(01)00602-1

Bergfreund, J., Sun, Q., Fischer, P., and Bertsch, P. (2019). Adsorption of Charged Anisotropic Nanoparticles at Oil-Water Interfaces. *Nanoscale Adv.* 1, 4308–4312. doi:10.1039/c9na00506d

Bertsch, P., Arcari, M., Geue, T., Mezzenga, R., Nyström, G., and Fischer, P. (2019). Designing Cellulose Nanofibrils for Stabilization of Fluid Interfaces. *Biomacromolecules* 20, 4574–4580. (2020). Adsorption and Interfacial Structure of Nanocelluloses at Fluid Interfaces. *Adv. Colloid Interf. Sci.* 276, 102089. doi:10.1016/j.cis.2019.102089

Blankart, M., Kratzner, C., Link, K., Oellig, C., Schwack, W., and Hinrichs, J. (2020). Technical Emulsifiers in Aerosol Whipping Cream - Compositional Variations in the Emulsifier Affecting Emulsion and Foam Properties. *Int. Dairy J.* 102, 104578. doi:10.1016/j.idairyj.2019.104578

Capron, I., Rojas, O. J., and Bordes, R. (2017). Behavior of Nanocelluloses at Interfaces. *Curr. Opin. Colloid Interf. Sci.* 29, 83–95. doi:10.1016/j.cocis.2017.04.001

Cervin, N. T., Andersson, L., Ng, J. B. S., Olin, P., Bergström, L., and Wågberg, L. (2013). Lightweight and strong Cellulose Materials Made from Aqueous Foams Stabilized by Nanofibrillated Cellulose. *Biomacromolecules* 14, 503–511. doi:10.1021/bm301755u

Cervin, N. T., Johansson, E., Benjamins, J.-W., and Wågberg, L. (2015). Mechanisms behind the Stabilizing Action of Cellulose Nanofibrils in Wet-Stable Cellulose Foams. *Biomacromolecules* 16, 822–831. doi:10.1021/bm5017173

Cha, J. Y., Chung, D. S., Seib, P. A., Flores, R. A., and Hanna, M. A. (2001). Physical Properties of Starch-Based Foams as Affected by Extrusion Temperature and Moisture Content. *Ind. Crops Prod.* 14, 23–30. doi:10.1016/s0926-6690(00)00085-6

Chinnaswamy, R. (1993). Basis of Cereal Starch Expansion. *Carbohydr. Polym.* 21, 157–167. doi:10.1016/0144-8617(93)90012-s

Cosgrove, D. J. (2005). Growth of the Plant Cell wall. *Nat. Rev. Mol. Cel Biol* 6, 850–861. doi:10.1038/nrm1746

Dufresne, A. (2012). *Nanocellulose: From Nature to High Performance Tailored Materials*. Munchen, Germany: Walter de Gruyter.

Dufresne, A. (2013). Nanocellulose: a New Ageless Bionanomaterial. *Mater. Today* 16, 220–227. doi:10.1016/j.mattod.2013.06.004

Ebringerová, A. (2005). Structural Diversity and Application Potential of Hemicelluloses. *Macromol. Symp.* 232, 1–12. doi:10.1002/masy.200551401

Fujisawa, S., Togawa, E., and Kuroda, K. (2017). Nanocellulose-stabilized Pickering Emulsions and Their Applications. *Sci. Tech. Adv. Mater.* 18, 959–971. doi:10.1080/14686996.2017.1401423

Gama, N., Ferreira, A., and Barros-Timmons, A. (2018). Polyurethane Foams: Past, Present, and Future. *Materials* 11, 1841. doi:10.3390/ma11101841

Ganesan, K., Budtova, T., Ratke, L., Gurikov, P., Baudron, V., Preibisch, I., et al. (2018). Review on the Production of Polysaccharide Aerogel Particles. *Materials* 11, 2144. doi:10.3390/ma11112144

Getz, C. A., Smith, G. F., Tracy, P. H., and Prucha, M. J. (1937). Instant Whipping of Cream by Aeration. *J. Food Sci.* 2, 409–428. doi:10.1111/j.1365-2621.1937.tb16532.x

Härdelin, L., Bernin, D., Börjesson, M., Ström, A., and Larsson, A. (2020). Altered Thermal and Mechanical Properties of Spruce Galactoglucomannan Films Modified with an Etherification Reaction. *Biomacromolecules* 21, 1832–1840. doi:10.1021/acs.biomac.9b01730

Hillis, W. E. (1984). High Temperature and Chemical Effects on wood Stability. *Wood Sci. Technol.* 18, 281–293. doi:10.1007/bf00353364

Hofmann, T., Linke, L., Tsiapouris, A., and Ziems, A. (1998). Porous Materials Made from Starch. *Chem. Eng. Technol.* 21, 580–584. doi:10.1002/(sici)1521-4125(199807)21:7<580:aid-ceat580>3.0.co;2-9

Jeon, B., Kim, H. K., Cha, S. W., Lee, S. J., Han, M.-S., and Lee, K. S. (2013). Microcellular Foam Processing of Biodegradable Polymers - Review. *Int. J. Precis. Eng. Manuf.* 14, 679–690. doi:10.1007/s12541-013-0092-0

Karlsson, K., Schuster, E., Stading, M., and Rigdahl, M. (2015). Foaming Behavior of Water-Soluble Cellulose Derivatives: Hydroxypropyl Methylcellulose and Ethyl Hydroxyethyl Cellulose. *Cellulose* 22, 2651–2664. doi:10.1007/s10570-015-0669-0

Kishani, S., Vilaplana, F., Xu, W., Xu, C., and Wågberg, L. (2018). Solubility of Softwood Hemicelluloses. *Biomacromolecules* 19, 1245–1255. doi:10.1021/acs.biomac.8b00088

Kistler, S. S. (2002). Coherent Expanded-Aerogels. *J. Phys. Chem.* 36, 52–64. doi:10.1021/j150331a003

Kuboki, T., Lee, Y. H., Park, C. B., and Sain, M. (2009). Mechanical Properties and Foaming Behavior of Cellulose Fiber Reinforced High-Density Polyethylene Composites. *Polym. Eng. Sci.* 49, 2179–2188. doi:10.1002/pen.21464

Kuboki, T. (2014). Mechanical Properties and Foaming Behavior of Injection Molded Cellulose Fiber Reinforced Polypropylene Composite Foams. *J. Cell Plastics* 50, 129–143. doi:10.1177/0021955x13504776

Lavoine, N., and Bergström, L. (2017). Nanocellulose-based Foams and Aerogels: Processing, Properties, and Applications. *J. Mater. Chem. A.* 5, 16105–16117. doi:10.1039/c7ta02807e

Lawoko, M. (2013). Unveiling the Structure and Ultrastructure of Lignin Carbohydrate Complexes in Softwoods. *Int. J. Biol. Macromolecules* 62, 705–713. doi:10.1016/j.ijbiomac.2013.10.022

Lehtonen, M., Merinen, M., Kilpeläinen, P. O., Xu, C., Willför, S. M., and Mikkonen, K. S. (2018). Phenolic Residues in spruce Galactoglucomannans Improve Stabilization of Oil-In-Water Emulsions. *J. Colloid Interf. Sci.* 512, 536–547. doi:10.1016/j.jcis.2017.10.097

Lehtonen, M., Teräslahti, S., Xu, C., Yadav, M. P., Lampi, A.-M., and Mikkonen, K. S. (2016). Spruce Galactoglucomannans Inhibit Lipid Oxidation in Rapeseed Oil-In-Water Emulsions. *Food Hydrocoll.* 58, 255–266. doi:10.1016/j.foodhyd.2016.03.006

Maleki, L., Edlund, U., and Albertsson, A.-C. (2017). Synthesis of Full Interpenetrating Hemicellulose Hydrogel Networks. *Carbohydr. Polym.* 170, 254–263. doi:10.1016/j.carbpol.2017.04.091

Maniglio, D., Bonani, W., Migliaresi, C., and Motta, A. (2018). Silk Fibroin Porous Scaffolds by N2O Foaming. *J. Biomater. Sci. Polym. Edition* 29, 491–506. doi:10.1080/09205063.2018.1423811

Marrazzo, C., Maio, E. D., and Iannace, S. (2016). Foaming of Synthetic and Natural Biodegradable Polymers. *J. Cell Plastics* 43, 123–133. doi:10.1177/0021955x06073214

Martoïa, F., Cochereau, T., Dumont, P. J. J., Orgéas, L., Terrien, M., and Belgacem, M. N. (2016). Cellulose Nanofibril Foams: Links between Ice-Templating Conditions, Microstructures and Mechanical Properties. *Mater. Des.* 104, 376–391. doi:10.1016/j.matdes.2016.04.088

Mikkonen, K. S., Tenkanen, M., Cooke, P., Xu, C., Rita, H., Willför, S., et al. (2009). Mannans as Stabilizers of Oil-In-Water Beverage Emulsions. *LWT - Food Sci. Tech.* 42, 849–855. doi:10.1016/j.lwt.2008.11.010

Mikkonen, K. S., Xu, C., Berton-Carabin, C., and Schroën, K. (2016). Spruce Galactoglucomannans in Rapeseed Oil-in-Water Emulsions: Efficient Stabilization Performance and Structural Partitioning. *Food Hydrocoll.* 52, 615–624. doi:10.1016/j.foodhyd.2015.08.009

Nypelö, T., Laine, C., Aoki, M., Tammelin, T., and Henniges, U. (2016). Etherification of Wood-Based Hemicelluloses for Interfacial Activity. *Biomacromolecules* 17, 1894–1901. doi:10.1021/acs.biomac.6b00355

O'neil, M. J., Smith, A., Heckelman, P. E., and Budavari, S. (2001). *The Merck index-An Encyclopedia of Chemicals, Drugs, and Biologicals*, 767. whitehouse station, NJ: Merck and Co. Inc, 4342.

Ottenhall, A., Seppänen, T., and Ek, M. (2018). Water-stable Cellulose Fiber Foam with Antimicrobial Properties for Bio Based Low-Density Materials. *Cellulose* 25, 2599–2613. doi:10.1007/s10570-018-1738-y

Palasingh, C., Ström, A., Amer, H., and Nypelö, T. (2021). Oxidized Xylan Additive for Nanocellulose Films - A Swelling Modifier. *Int. J. Biol. Macromolecules* 180, 753–759. doi:10.1016/j.ijbiomac.2021.03.062

Sehaqui, H., Salajková, M., Zhou, Q., and Berglund, L. A. (2010). Mechanical Performance Tailoring of Tough Ultra-high Porosity Foams Prepared from Cellulose I Nanofiber Suspensions. *Soft Matter* 6, 1824–1832. doi:10.1039/b927505c

Sehaqui, H., Zhou, Q., and Berglund, L. A. (2011). High-porosity Aerogels of High Specific Surface Area Prepared from Nanofibrillated Cellulose (NFC). *Composites Sci. Tech.* 71, 1593–1599. doi:10.1016/j.compscitech.2011.07.003

Sixta, H. (2006). *Handbook of Pulp*. Wiley VCH.

Soykeabkaew, N., Thanomsilp, C., and Suwantong, O. (2015). A Review: Starch-Based Composite Foams. *Compos. Part A Appl. Sci. Manuf.* 78, 246–263. doi:10.1016/j.compositesa.2015.08.014

Stankov, S., Fidan, H., Hristov, T., and Nikovska, K. (2021). Physical and Sensory Characteristics of Edible Foams Obtained with Nitrous Oxide. *IOP Conf. Ser.: Mater. Sci. Eng.* 1031 (1), 012115. doi:10.1088/1757-899X/1031/1/012115

Svagan, A. J., Samir, M. A. S. A., and Berglund, L. A. (2008). Biomimetic Foams of High Mechanical Performance Based on Nanostructured Cell Walls Reinforced by Native Cellulose Nanofibrils. *Adv. Mater.* 20, 1263–1269. doi:10.1002/adma.200701215

Wemmer, J., Gossweiler, E., Fischer, P., and Windhab, E. J. (2019). Effect of Foaming on Mechanical Properties of Microfibrillated Cellulose-Based Porous Solids. *Cellulose* 26, 2487–2497. doi:10.1007/s10570-018-02228-5

Willför, S., Rehn, P., Sundberg, A., Sundberg, K., and Holmbom, B. (2003). Recovery of Water-Soluble Acetylgalactoglucomannans from Mechanical Pulp of spruce. *Tappi J.* 2, 27–32.

Xie, Y., Tong, Q., Chen, Y., Liu, J., and Lin, M. (2011). Manufacture and Properties of Ultra-low Density Fibreboard from wood Fibre. *BioResources* 6, 4055–4066.

Xu, C. L., Willfor, S., Sundberg, K., Petterson, C., and Holmbom, B. (2007). Physico-chemical Characterization of spruce Galactoglucomannan Solutions: Stability, Surface Activity and Rheology. *Cellulose Chem. Tech.* 41, 51–62.

Yokozeki, A., and Shiflett, M. B. (2011). The Solubility of CO_2 and N_2O in Olive Oil. *Fluid Phase Equilib.* 305, 127–131. doi:10.1016/j.fluid.2011.03.013

Conflict of Interest: The authors declare that the research was conducted in the absence of any commercial or financial relationships that could be construed as a potential conflict of interest.

Publisher's Note: All claims expressed in this article are solely those of the authors and do not necessarily represent those of their affiliated organizations, or those of the publisher, the editors, and the reviewers. Any product that may be evaluated in this article, or claim that may be made by its manufacturer, is not guaranteed or endorsed by the publisher.